Global NEST Journal, Vol 25, No 2, pp 95-105

An innovative solution for the treatment of poultry industry wastewater with advanced hybrid technology sono-photocatalysis

Dogdu G.* and Sen N.E.
Department of Environmental Engineering, Bolu Abant Izzet Baysal University, Bolu, Turkey
Received: 18/03/2022, Accepted: 12/08/2022, Available online: 24/08/2022
*to whom all correspondence should be addressed: e-mail: gamzedogdu@ibu.edu.tr
https://doi.org/10.30955/gnj.004305

Graphical abstract

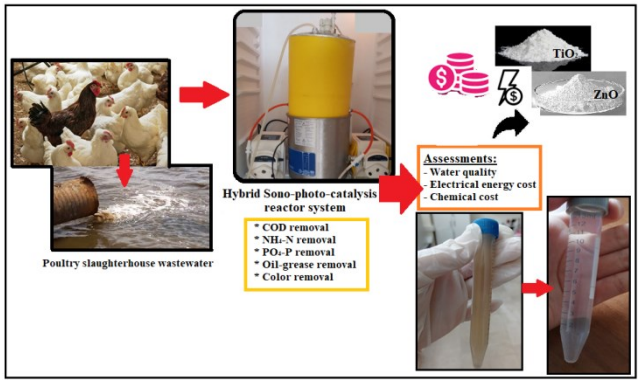

Abstract

Poultry slaughterhouse wastewater (PSWW) is a crucial concern fundamentally due to extensive generation and related substantial amounts of recalcitrant organic content due to high COD and oil and grease (O&G) levels. Hybrid advanced oxidation processes are promising, green, and innovative options to treat various industrial wastewater; to date, this potential has not been implemented to high-strength wastewater from the poultry industry. This work aims to investigate the combination of ultrasound and photocatalysis processes in the treatment of poultry slaughterhouse wastewater for the removal of COD and O&G under different operating conditions such as catalyst type (TiO_2 and ZnO), irradiation type (UVA_{365} and UVC_{254}), catalyst dosage (0.5-2.5 g/L), pH (2–10), hydrogen peroxide concentration (0-10 mM) and operation time (30-180 min). Taguchi's experimental design based on the L_{36} orthogonal array was adequately applied to optimize the process. The finding results presented that ZnO concentration of 2.5 g/L, pH 2, and operation time of 180 min under UVC_{254} were optimum parameters to achieve maximum COD removal while, ZnO concentration of 1.5 g/L, pH 6, H_2O_2 concentration of 5 mmol/L and operation time of 30 min under UVC_{254} were optimum parameters to achieve maximum oil and grease removal. With these optimum conditions, the best attained COD and O&G removal yields were 54% and 99%, respectively.

Keywords: Optimization, poultry slaughterhouse wastewater, Sonophotocatalysis, synergetic effect, Taguchi method

1. Introduction

The poultry meat sector is accepted as one of the largest and rapidly growing agro-based industries in many parts of the world due to being an affordable and nutritious protein source (Ngobeni *et al.*, 2022; Hilares *et al.*, 2021). Despite high economic gains, poultry processes such as slaughtering, de-feathering, evisceration trimming, and washing are extremely water-intensive processes, consuming an averagely of 26.5 L per bird (Fatima *et al.*, 2021). PSWW contains different complex organic and inorganic substances such as blood, fat oil and grease (FOG), protein, heavy metals, and detergents for cleaning, as well as high concentrations of nutrients such as nitrogen (N) and phosphorus (P), chemical oxygen demand (COD), biochemical oxygen demand (BOD), suspended and dissolved solids and pathogens (Bustillo-Lecompte *et al.*, 2016). FOG can be a crucial problem for wastewater treatment because of their slow decomposition (Gaur *et al.*, 2010). Especially for biological treatment systems, biodegradation activity can be hindered due to clogging and blockage of the piping system and encapsulation of the granules in the presence of FOG (Bingo *et al.*, 2021). Besides, the discharge of untreated poultry wastewater into the receiving environment creates both eutrophication and over-fertilization of soils. Moreover, it causes infection-related health risks for humans and animals using contaminated water, as well as problems such as congestion and foam formation in the drainage systems of wastewater treatment plants, due to excess nitrogen and phosphorus in their content (Cao *et al.*, 2021; Garcia *et al.*, 2020). Therefore, the urgency to develop an efficient, environmentally friendly and innovative advanced treatment technology to reach specific discharge limits and to ensure sustainable economic growth is inevitable (Dyosile *et al.*, 2021).

Recently, several advanced oxidation processes (AOPs) have been explored for the treatment of PSWW, i.e., electrocoagulation (Potrich *et al.*, 2020; Emerick *et al.*, 2020), Fenton (Cui *et al.*, 2021), electro-Fenton (Zhang *et*

al., 2020), ultrasound (Abdelhay *et al.*, 2020) and photocatalysis (Samsudin *et al.*, 2019; Asha and Kumar, 2015); however, to the best of our knowledge, there has yet been no published researches have been established on the synergistic effect of combined photocatalysis and sonolysis processes called "sono-photocatalysis" (SPC) for the PSWW treatment. The hybrid SPC technique has gained much popularity to perfectively degrade all kinds of pollutants in extending the photogenerated electron-hole transfer pathway owing to easy operational, cheapness, and rapid pollution-free technology (Khan *et al.*, 2022; Karim and Shriwastav, 2020; Fan *et al.*, 2022). Besides, critical limitations, including the required long reaction time for the single process and their low capability to achieve complete mineralization of organic molecules for their individual use can be eliminated by the combination of photon, ultrasonic waves, and a semiconductor catalyst (Abdurahman *et al.*, 2021; Khitab *et al.*, 2022).

Although several kinds of research have been reported so for concerning the photocatalytic activity of TiO_2 (~3.2 eV) and ZnO (~3.37 eV), which are widely used functional semiconductors that are chosen for their low cost, chemical stability, non-toxicity, and higher photosensitive properties (Stando *et al.*, 2021; Boutra *et al.*, 2021), as the first time, the comparison performances of these two catalysts on the treatment of PSWW were widely explored in this work. Also, treatment efficiencies of SPC for PSWW under UVA_{365} and UVC_{254} irradiations have not been studied by any researchers, which was investigated in this study. Moreover, hydrogen peroxide (H_2O_2) is a strong oxidant, which enhances the generation of HO. and pollutant degradation is rarely reported in the SPC process (Wei *et al.*, 2021; Silva *et al.*, 2007). In this work, the effect of H_2O_2 concentration and was evaluated in detail. Taguchi's experimental design based on orthogonal array (OA) analysis was used to determine the contribution of each factor, optimal condition and the response with least number of tests, time, and experiment cost (Fard *et al.*, 2020) in various treatment processes from industrial wastewater. Nonetheless, based on an extensive literature survey, research on the application of Taguchi's method for PSWW treatment using the SPC technique has not been available. Therefore, to address these knowledge gaps, the primary aim of this study was to optimize the individual and interactive effect of process variables such as catalyst type and dosage of catalysts (TiO_2 and ZnO), pH of solution, H_2O_2 concentration, ultraviolet (UV) irradiation type (UVA_{365} and UVC_{254}) and operation time on the COD and oil and grease from PSWW using Taguchi experimental design with L_{36} (2^2 x 3^4) orthogonal array.

2. Materials and methods

2.1. Poultry slaughterhouse wastewater

The poultry slaughterhouse wastewater (PSWW) used in the present study was collected from a local integrated poultry processing plant, which has a capacity of 180.000/chicken and produces an averagely of 1300-1500 m^3 wastewater per day located at Bolu, Turkey. The sample was taken from the effluent pipe of the slaughterhouse unit of the plant. After collection, the samples were stored at 4 ºC in dark conditions. Raw poultry wastewater samples were filtered to remove feather, bone, and meat particles before each experiment. The chemical analysis of PSWW was shown in Table 1.

2.2. Chemicals

The nano-sized photocatalysts, TiO_2 (AEROXIDE® P25 ≥ %99,5, anatase form, 21 nm, 35–65 m^2/g BET surface area) and ZnO (<5 µm particle size, %99,9; <10-25 m^2/g) were supplied from Sigma-Aldrich (Germany). H_2O_2 (30%), used as an oxidizing agent, was also obtained from Sigma-Aldrich (Germany). Sodium hydroxide (NaOH, 99% purity) and sulfuric acid (H_2SO_4, 97% purity) were obtained from Merck (Germany) to ensure the desired pH conditions in the experiments. All chemicals were used without additional purification. During the experiments, deionized water was used to prepare the necessary solutions (Merck Milli-Q, Germany, spec. resistivity: 18.2 MΩ).

2.3. Experimental set-up and procedure

A schematic of SPC reactor used in this work is shown in Figure 1. All ultrasound, photocatalytic, and sono-photocatalytic experiments were performed using the same cylindrical Pyrex glass immersion well reactor filled with 200 mL solution with a certain amount of catalyst. The batch-mode reactor was equipped with a water jacket and a PL-L UVA_{365} lamp (Philips, Dutch) (360 W; 315 to 380 nm; 110 µW/cm^2), and a UVC_{254} lamp (Philips, Dutch) (9 W; 254 nm) were used to study the SPC method. Air at 3.5 L/min was supplied to the reactor system using a diffuser. For the US experiments, the whole photoreactor system was immersed in an ultrasonic bath (Bandelin DT 106, Germany) with a capacity of 5.6 L (operating volume, 200 mL), a tank size of D = 240 mm, and L = 125 mm, and an operating frequency of 35 ± 3 kHz (120 W, 220 V) that was equipped with the in-built piezoelectric transducer placed at the bottom and an external generator was used. The reactor temperature was kept constant at 25 ± 3 °C with a continuous water bath (NUVE ST-30, Turkey) and a cold water pump (Filtec PH-15X3S-FPP-1, Germany).

2.4. Analytical methods

PSWW samples were taken at the beginning and end of each experiment run, centrifuged at 5000 rpm for 15 min, and filtered using 0.45 µm filters (Minisart RC25, Sartorious) to remove catalysts. O&G was measured according to standard method 1164, EPA with hexane extraction. COD values before and after treatment were measured by (Merck Spectroquant Pharo100) spectrophotometer that was adapted for the Standard Method for Water and Wastewater (APHA, AWWA & WEF, 2012). COD was determined in the influent and effluent of the reactor samples using the Merck spectroquant COD cell test kits, respectively. When the sample containing hydrogen peroxide (H_2O_2), interference in COD determination was reduced by increasing the pH to above 10 to decompose the hydrogen peroxide to oxygen and water (Talinli and Anderson, 1992). The pH of the wastewater was adjusted either using 0.1 M concentrated H_2SO_4 or 0.1M NaOH. Electrical conductivity (EC), redox potential, and pH of the wastewater were determined by

direct measurement using Termo Orion 5 Star multimeter device. The reactor was operated in a batch mode for 180 min when was needed to reach steady-state COD readings according to preliminary studies. Each experiment was conducted twice, the pollutant concentrations were measured from influent and effluent from the reactor system each time and the average results were given in this study. The pollutant removal efficiency was calculated as the following formula:

$$R(\%) = 100\% \times (C_i - C_f)/C_i \quad (1.1)$$

where, C_i and C_f represent the mean values of initial concentration and final concentration after treatment, respectively.

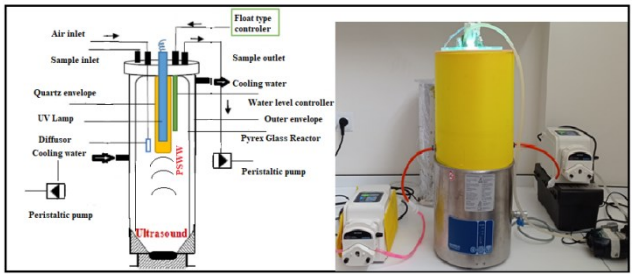

Figure 1. Experimental setup for the hybrid sonophotocatalysis (SPC) process.

Table 1 The characterization of raw poultry slaughterhouse wastewater (PSWW)

Parameter	Unit	Value
pH	-	7.37 ± 0.03
Temperature	ºC	23.0 ± 0.06
Redox potential	mV	25.7 ± 0.38
Electrical conductivity	µS/cm	1356 ± 2.65
Turbidity	NTU	722 ± 2.52
Color	Pt/Co	6127 ± 46.0
Oil & grease	mg/L	5647 ± 19.3
Suspended solids	mg/L	493 ± 2.52
COD	mg/L	3280 ± 39.1
NH_4-N	mg/L	95 ± 5.00
NO_2-N	mg/L	6.67 ± 0.15
NO_3-N	mg/L	30.0 ± 1.00
PO_4-P	mg/L	105 ± 2.00
Physical appearance	-	Reddish brown
T-N	mg/L	305 ± 5.00
T-P	mg/L	47.7 ± 1.53

Table 2. Experimental factors and design levels of orthogonal array

Code	Symbol	Factors	Unit	Level 1	Level 2	Level 3
A	C_T	Catalyst type	-	TiO_2	ZnO	-
B	UV_T	UV irradiation type	-	UVA_{365}	UVC_{254}	-
C	C_C	Catalyst concentration	g/L	0.5	1.5	2.5
D	pH	pH	-	2	6	10
E	C_{H2O2}	H_2O_2 concentration	mmol/L	0	5	10
F	t	Time	min	30	105	180

2.5. Taguchi experimental design

To identify and optimize the process parameters on the selected response though the use of analysis of variance (ANOVA), Taguchi's design of experiments (DOE) approach was conducted by employing a minimum number of the test via orthogonal arrays (OA) (Aydıner *et al.*, 2019). In this study, Taguchi's approach with six controllable factors (A: catalyst type (C_T), B: UV irradiation type (UV_T), C: catalyst concentration (C_C), D: pH, E: H_2O_2 concentration (C_{H2O2}), F: operation time (t) were chosen for investigating SPC process. The levels of the factors used in the process were selected according to the literature review (Ayare and Gogate, 2020; Karim and Shriwastav, 2020; Steven *et al.*, 2021; Khan *et al.*, 2022). Table 2 shows the Taguchi L_{36} (2^2 x 3^4) orthogonal array that defines a total of 36 experimental sets, two independents with two levels and four independents with three levels used in the study. Minitab 17.0 Statistical Software was applied for optimization and statistical analysis. COD and O&G removal yields were chosen as two responses for investigating the hybrid SPC method. The signal/noise ratio (S/N) defines the measurement of the deviation of the response from the desired value (Fdez-Sanromán *et al.*, 2021). While the mean value shows ''signal'' that represents the desirable effect, the standard deviation indicates ''noise'' represents the undesirable effect of the data set measured by the S/N ratio (Sohrabi *et al.*, 2017).

To achieve maximum pollutant removal performance with lower variability in the process, the "largest best" (eqn. 2.1) S/N ratio was chosen (Abbas and Abbas, 2021):

$$\frac{S}{N}[dB] = -10\log\left[\frac{1}{n}\sum_{i=1}^{n}\frac{1}{Y_i^2}\right] \quad (2.1)$$

where n is the number of experimental replicates and Y_i is defined as the performance value of the i^{th} experiment.

3. Results and discussion

3.1. Performance of individual AOPs and synergistic effect

Several energy-based AOPs, namely UVA_{365}, UVC_{254}, US, TiO_2, ZnO, and H_2O_2 oxidation were applied individually to attain the oxidation potential in terms of COD removal from PSWW for 180 min under the same operation conditions as shown in Table 3.

Table 3. COD removal efficiencies resulting from using a variety of individual and combined processes (35 kHz US frequency; 120 W US power; pH 6; 1.5 g/L catalyst concentration; 10 mmol/L H_2O_2 concentration; 36 W UV power; 25 ± 3 °C temperature; 180 min)

Advanced oxidation treatment method	COD removal (%)
Ultraviolet A (UVA_{365})	5 ± 0.08
Ultraviolet A (UVC_{254})	7 ± 0.01
Ultrasound (US)	5 ± 0.16
TiO_2	6 ± 0.01
ZnO	9 ± 0.1
H_2O_2	6 ± 0.24
UVA_{365}+TiO_2	16 ± 0.01
UVA_{365}+ZnO	19 ± 0.22
UVC_{254}+TiO_2	22 ± 0.07
UVC_{254}+ZnO	28 ± 0.02
US+UVA_{365}+TiO_2	22 ± 0.74
US+UVC_{254}+TiO_2	30 ± 0.85
US+UVA_{365}+ZnO	33 ± 0.34
US+UVC_{254}+ZnO	47 ± 0.30

The preliminary experiments suggest that the COD removal efficiencies were 5%, 5%, 7%, 6%, 9%, and 6% using sonolysis (US), photolysis (P) (UVA_{365} and UVC_{254}), catalysis (TiO_2 and ZnO) and oxidation, respectively. It was observed that none of the individual processes were capable of satisfactory COD removal from PSWW. Similar to our findings, Al-Bsoul *et al.*, (2020) stated that only 3% sono-photocatalytic oxidation of olive mill wastewater (OMW) was achieved after UV treatment for 180 min versus 5% obtained with ultrasound. Especially at low frequencies, the formation of highly hydrophilic intermediates via HO. the attack leads to a long sonochemical degradation time to achieve complete mineralization (Ahmedchekkat *et al.*, 2011). Wei *et al.*, (2021) indicated that sono-photocatalytic degradation efficiencies of acid orange 7 (AO7) dye were 3.61%, 8.14%, 1.15%, and 1.97% using sonolysis, photolysis, catalysis, and oxidation, respectively. Kakavandi and Ahmadi (2019) declared that the minimum efficiencies for single sonolysis or photolysis could allude to by the lower generation rate of free radicals in the whole system. Coupling the UV irradiations with TiO_2 and ZnO catalysts called "photocatalysis (PC)" significantly improved the removal rate of COD (between 16% and 28%) due to the excellent activation capability of TiO_2 and ZnO under UV irradiations (Yang *et al.*, 2021). Higher oxidation resulted with the absorbance of incident light by semiconductors. Consequently, higher energy photo-induced electrons (e^-) and holes (h^+) were generated which migrated to the catalyst surface and produced reactive oxygen radicals (ROS) that participated in oxidation reaction with pollutants (Patidar and Srivastava, 2021).

For the hybrid system, the introduction of US with UVA_{365}/TiO_2, UVC_{254}/TiO_2, UVA_{365}/ZnO, and UVC_{254}/ZnO significantly improved the COD removal efficiencies by 22%, 30%, 33%, and 47%, respectively. The synergy index is the ratio of the hybrid SPC removal percentage value to the sum of the individual processes' removal percentage values with regard to COD removal. The synergy was calculated to determine the system's synergy according to eqn. 3.1 (Poblete *et al.*, 2020):

$$\text{Synergy index} = \frac{\text{Removal of pollutants with US and PC}}{\text{Removal of pollutants with PC} + \text{Removal of pollutants with US}} \quad (3.1)$$

For the oxidation of PSWW, the observed synergy index values for the combined US/UVA_{365}/TiO_2, US/UVC_{254}/TiO_2, US/UVA_{365}/ZnO, and US/UVC_{254}/ZnO were obtained as 1.05, 1.11, 1.38 and 1.42, respectively. Kakavandi and Ahmedi (2019) proposed that synergy index (R) equals to 1 and R > 1.0 implies the integrated effect was greater than the sum of all individual effects and the combination of photocatalysis (PC) and ultrasound processes (US) exhibited higher oxidation performance of PSWW when compared with individual processes. The combination of two systems into one system enhances the amount of HO. radicals formed as a result of the increment in the surface area of the catalyst that accelerates the degradation of organic pollutants as indicated by Al-Bsoul *et al.*, (2022). The cavitation energy followed by its transformation into microbubbles is generated by ultrasonic waves which produce effectively higher localized temperature and pressure that destroy water molecules and produce additional hydroxyl radical HO., respectively. The additional hydroxyl free radical HO. formation along with

superoxide radical ($O_2^{\bullet-}$) helps in the improvement of the photodegradation ability of SPC (Khan *et al.*, 2022). Secondly, US conditions help to improve the dispersal of nanoparticles by preventing agglomeration, thus generation of radicals could be increased with higher catalyst active sections exposed (Babu *et al.*, 2019). So, the US can enable to increase the photocatalytic reaction rate by the catalytic activity of the catalyst. Also, acoustic cavitation cleans the catalyst surface and mass transfer induced by the US is accelerated between the solution and catalyst, which might lead to an increase in the photocatalytic degradation rate (Van de Moortel *et al.*, 2020).

3.2. Taguchi analysis to determine optimum parameters

Taguchi L_{36} design with the mean S/N ratios for each parameter level and removal efficiencies of COD and O&G are shown in Table 4. Since "larger-the-better" criteria were chosen for S/N ratios to achieve maximum removal yield, the highest values were optimum values. While COD removal efficiencies were between 15% and 54%, O&G removal efficiencies changed between 68% and 99%. Taguchi response table was used to determine the most effective process parameter between C_T, UV_T, C_C, pH, $C_{H_2O_2}$, and t for optimum COD removal efficiency level. S/N ratios were calculated using Eq. 2 are given in Table 5.

Operating conditions for the highest COD removal were obtained as A_2, B_2, C_3, D_1, E_1, and F_3 as presented in Table 5. The optimum parameters for COD removal efficiency were A (catalyst type) at level 2 (ZnO), B (UV irradiation type) at level 2 (UVC_{254}), C (catalyst concentration) at level 3 (2.5 g/L), D (pH) at level 1 (2), E (H_2O_2 concentration) at level 1 (0 mmol/L) and F (time) at level 3 (180 min), respectively. According to optimum conditions, COD removal efficiency was obtained as 54%.

In the present study, the importance of operating parameters on O&G removal efficiency was analyzed and S/N ratios were obtained are given in Table 5. Since 'the largest is the best' criteria were chosen, the highest values were optimum values. O&G removal efficiencies were between 68% and 99%. The optimum conditions were obtained as A_2, B_2, C_2, D_2, E_2, and F_1 for O&G removal. The optimum parameters for O&G removal efficiency were A (catalyst type) at level 2 (ZnO), B (UV irradiation type) at level 2 (UVC_{254}), C (catalyst concentration) at level 2 (1.5 g/L), D (pH) at level 2 (6), E (H_2O_2 concentration) at level 2 (5 mmol/L) and F (time) at level 1 (30 min), respectively. Under optimum conditions, O&G removal was obtained as 99%. These results showed that the optimum operating parameters' values changed according to the pollutant parameter, even if the same type of wastewater and reactor system were used as expressed by Adar and Acar (2021). It was observed that complete COD mineralization was more difficult and required a long time than O&G removal. Hence, the system should be optimized in terms of COD removal.

3.3. Statistical analysis

Table 6 gives the analysis of variance (ANOVA) results revealing the effects on COD and O&G removal efficiencies of the control factors of C_T, UV_T, C_C, pH, $C_{H_2O_2}$, and t at the confidence level of 95% and a significance level of $\alpha = 0.05$. The analysis was evaluated for α=0.05 significance level. As given in Table 6, the errors were 8.6% and 22.37% (<50%) for COD and O&G removal, respectively which were well below the limit value. This implied that the errors of the experiments were insignificant. Further, the quantitative assessment can be obtained using the percentage contribution rate (C_r %) (Yildiz, 2008). According to these results, the most important parameters for COD removal efficiency were presented as catalyst type (F: 230.2, C_r: 79%) > operation time (F:8.75 C_r: 6.02%) > UV lamp type (F: 5.46, C_r: 1.88%), respectively as shown in Table 6. However, the contributions of catalyst concentration (F: 2.4, C_r: 1.65%), pH (F: 2.61, C_r: 1.8%) and H_2O_2 concentration (F: 3.33, C_r:0.92%) were statistically insignificant ($p > \alpha$) in COD removal by SPC process. Besides, pH (F: 29.93, C_r: 54%) and operation time (F: 9.22, C_r: 17%) were the most significant factors ($p<\alpha$) in the removal efficiency of O&G in the SPC process.

3.4. Effects of operating parameters on COD and O&G removal efficiencies

3.4.1. Catalyst type effect

The main effect graph of the process parameters on the removal efficiencies of COD and O&G in real poultry slaughterhouse effluent is clearly shown in Figure 2. As shown in Figure 2(a-b), the sono-photocatalytic performance of the ZnO catalyst was found to be strongly higher than the TiO_2 catalyst in removing COD and O&G from raw PSWW, especially for the degradation of organic oil molecules due to its excellent catalytic activity, low-cost, non-toxicity, super hydrophilicity properties (Zioui *et al.*, 2019). For the elimination of O&G from wastewater, TiO_2 and ZnO catalysts play an important role in two removal mechanisms: (1) the interaction of oil on the adsorbent surface by adsorption that depends on the physical trapping of oil molecule on the adsorbent surface (Cui *et al.*, 2014); (2) photocatalysis for the separation of oil/water emulsion. TiO_2 or ZnO catalysts can be adsorbed on the interfacial surface between the oil and water when the oil in the water emulsion is blended with a photocatalyst. The surface of an organic emulsifier can be oxidized by the hydroxyl radicals between water and oil that are resulted in the destruction of the interfacial film structure (Liang and Esmaeili, 2021). Although ZnO has a similar band gap energy (3.37 eV) to TiO_2, the stability and electron mobility of ZnO (~100 cm^2/Vs) is twice that of TiO_2 (>1cm^2/Vs) (Gole *et al.*, 2017). Patidar and Srivastava (2021) also reported similar results during the sono-photocatalytic degradation of ofloxacin (OFLX) with 0.4 g/L ZnO catalyst under 40 kHz frequency, 125 W UV power at pH 6.3 within 120 min. Under UVA_{365}/US/TiO_2 process, OFLX mineralization efficiency was 24.1% while, 36.2% was obtained under UVA_{365}/US/ZnO system. The reason for the higher performance of the ZnO catalyst in comparison to the TiO_2 is due to the absorption of more light quanta as the quantum efficiency of the ZnO photocatalyst is higher than TiO_2 (Patidar and Srivastava, 2021). Besides, the ZnO catalyst is thought to have a lower light-scattering effect

due to its lower refractive index (ZnO: 2.0, TiO_2: 2.5-2.7) which also favors better photocatalytic efficiency (Jyothi *et al.*, 2015).

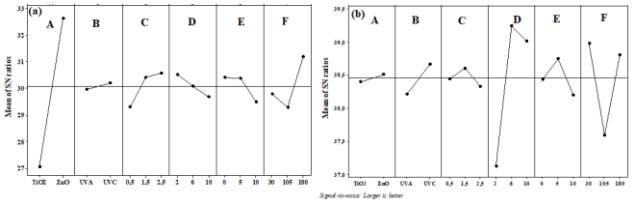

Figure 2. Main effects plot for S/N ratios with the larger-the better criteria of pollutant (a: COD, b: O&G) removal efficiencies (A: catalyst type, B: UV irradiation type, C: catalyst concentration, D: pH, E: H_2O_2 concentration, F: operation time).

Table 4. System performances obtained for all response parameters in SPC process

							COD removal		O&G removal	
No.	**C_T**	**UV_T**	**pH**	**C_C (g/L)**	**C_{H2O2} (mmol/L)**	**t (min)**	**Percentage (%)**	**S/N (db)**	**Percentage (%)**	**S/N (db)**
1	TiO_2	UVA	2	0.5	0	30	17.15	25.87	77.66	37.80
2	TiO_2	UVA	6	1.5	5	105	20.83	26.80	88.49	38.90
3	TiO_2	UVA	10	2.5	10	180	22.87	26.84	83.20	38.42
4	TiO_2	UVA	2	0.5	0	30	23.69	25.87	77.65	37.80
5	TiO_2	UVA	6	1.5	5	105	23.12	26.80	87.66	38.90
6	TiO_2	UVA	10	2.5	10	180	21.19	26.84	83.48	38.42
7	TiO_2	UVA	2	0.5	5	180	19.32	25.72	78.14	37.86
8	TiO_2	UVA	6	1.5	10	30	21.62	26.70	90.29	39.11
9	TiO_2	UVA	10	2.5	0	105	21.54	26.66	77.90	37.83
10	TiO_2	UVC	2	0.5	10	105	18.86	25.51	55.25	34.85
11	TiO_2	UVC	6	1.5	0	180	29.28	29.33	90.25	39.11
12	TiO_2	UVC	10	2.5	5	30	24.46	27.77	95.14	39.57
13	TiO_2	UVC	6	0.5	10	30	15.06	23.56	86.10	38.70
14	TiO_2	UVC	10	1.5	0	105	17.59	24.90	89.46	39.03
15	TiO_2	UVC	2	2.5	5	180	32.86	30.33	80.22	38.09
16	TiO_2	UVC	6	0.5	10	105	20.78	26.35	91.64	39.24
17	TiO_2	UVC	10	1.5	0	180	30.98	29.82	98.51	39.87
18	TiO_2	UVC	2	2.5	5	30	30.26	29.62	75.45	37.55
19	ZnO	UVA	6	0.5	0	180	47.29	33.49	94.45	39.50
20	ZnO	UVA	10	1.5	5	30	39.79	32.00	92.18	39.30
21	ZnO	UVA	2	2.5	10	105	36.96	31.35	71.45	37.08
22	ZnO	UVA	6	0.5	5	180	50.53	34.07	94.65	39.52
23	ZnO	UVA	10	1.5	10	30	34.67	30.80	97.11	39.74
24	ZnO	UVA	2	2.5	0	105	45.13	33.09	59.68	35.52
25	ZnO	UVA	10	0.5	5	30	36.12	31.15	93.05	39.37
26	ZnO	UVA	2	1.5	10	105	40.32	32.11	55.48	34.88
27	ZnO	UVA	6	2.5	0	180	43.51	32.77	82.16	38.29
28	ZnO	UVC	10	0.5	5	105	37.39	31.45	84.13	38.50
29	ZnO	UVC	2	1.5	10	180	52.00	34.32	86.90	38.78
30	ZnO	UVC	6	2.5	0	30	40.41	32.13	97.50	39.78
31	ZnO	UVC	10	0.5	10	180	46.11	33.28	96.85	39.72
32	ZnO	UVC	2	1.5	0	30	53.63	34.59	81.36	38.21
33	ZnO	UVC	6	2.5	5	105	40.44	32.14	98.50	39.87
34	ZnO	UVC	10	0.5	0	105	38.75	31.76	77.46	37.78
35	ZnO	UVC	2	1.5	5	180	45.42	33.14	76.50	37.67
36	ZnO	UVC	6	2.5	10	30	47.54	33.54	95.80	39.63

3.4.2. Irradiation type effect

As shown in Figure 2(a-b), the removal of COD from PSWW by using UVA (320-400 nm) and UVC (253.7 nm) radiation was investigated and UVC radiation showed statistically significant performance in comparison with UVA ($p=0.028$, $p<\alpha$). According to photon theory and Planck's eqn. 3.2:

$$E = hC/\lambda \quad (3.2)$$

h is Planck's constant (6.626×10^{-34} Js), c is the speed of light (3×10^8 m/s) and λ defines the cut-off wavelength, respectively. The wavelength is inversely proportional to the energy, thus shorter wavelength has a higher energy that results in increased activity and a higher probability of

photocatalytic reaction (Termtanun, 2013). Bushnaq (2006) stated that under UVC irradiation, atrazine was degraded by direct photolysis by about 95% within 60 min compared with 10% UVA irradiation. Besides, in the presence of 15 mg/L, atrazine removal was obtained as 84% by UVC irradiation compared with UVA in the presence of 25 mg/L TiO_2 catalysts after 60 min of irradiation. TiO_2 could absorb light at a lower wavelengths better than at a higher wavelength, hence UVC with a shorter wavelength corresponds to higher photon energy (Termtanun, 2013). Similarly, Yatmaz and Sen (2018) explained that homogeneous and heterogeneous photo-Fenton with the use of mineral catalysts achieved higher dye removal under UVC irradiation in comparison to those under UVA and mineral catalysts gave shorter removal times under UVC than under UVA.

3.4.3. Catalyst concentration effect

The effect of three catalyst dosages of 0.5 g/L, 1.5 g/L, and 2.5 g/L on the COD and O&G degradation were investigated for TiO_2 and ZnO catalysts, respectively as given in Figure 2(a-b). As expected, with an increase in catalyst dosage, percentage removal efficiencies of COD and O&G increase up to 1.5 g/L which is due to the maximum number of active sites available with more photo-generated electron holes for the generation of maximum active species during the degradation of organic pollutants (Abdelhay *et al.*, 2020; Khan *et al.*, 2022). Also, increasing catalyst concentration causes an increase in the number of cavitation bubbles due to providing additional nuclei, and consequently, more HO. radicals are generated in the bulk solution (Fan *et al.*, 2022; Karim and Shriwastav, 2020). Nevertheless, for doses greater than 1.5 g/L, more catalyst aggregation will occur and the number of active sites decreases that resulting in inhibition of light penetration, and the loss of active sites depends on shielding effects, generating HO. in the solution (Boutra *et al.*, 2021). Furthermore, Hapeshi *et al.*, (2013) declared that the ultrasound waves are scattered due to the use of a sonocatalyst in the system resulting in a lower amount of energy. Less amount of ultrasonic irradiation could be passed into the system because of the dominancy of the scattering of sound waves, in the presence of a higher dosage of catalyst.

Table 5. S/N response table for response parameters in SPC system (%)

	COD Removal (%)							O&G Removal (%)					
	C_T	UV_T	C_C	pH	C_{H2O2} (mmol/L)	t (min)		C_T	UV_T	C_C	pH	C_{H2O2} (mmol/L)	t (min)
Level	**A**	**B**	**C**	**D**	**E**	**F**	Level	**A**	**B**	**C**	**D**	**E**	**F**
1	27.05	29.96	29.29	30.51	30.4	29.79	1	38.39	38.21	38.44	37.12	38.43	38.98
2	32.62	30.2	30.41	30.08	30.38	29.29	2	38.51	38.66	38.60	39.24	38.74	37.59
3			30.57	29.68	29.49	31.19	3			38.33	39.01	38.2	38.8
Delta	5.57	0.24	1.28	0.84	0.92	1.91	Delta	0.11	0.45	0.27	2.12	0.55	1.39
Rank	1	6	3	5	4	2	Rank	6	4	5	1	3	2

Table 6. ANOVA results for performance parameters in SPC system

Source	Sum of squares	Degree of freedom	Mean square	F value	p value	Contribution (%)	Source	Sum of squares	Degree of freedom	Mean square	F value	p value	Contribution (%)
COD removal (%)							**O&G removal (%)**						
A	3691.21	1	3691.21	230.2	0.000	**79.14**	A	22.92	1	22.92	0.57	0.459	0.51
B	87.63	1	87.63	5.46	0.028	1.88	B	145.24	1	145.24	3.59	0.070	3.22
C	76.97	2	38.49	2.4	0.111	1.65	C	53.22	2	26.61	0.66	0.527	1.18
D	83.87	2	41.93	2.61	0.093	1.8	D	2420.67	2	1210.34	29.93	0.000	**53.59**
E	42.74	2	21.37	1.33	0.282	0.92	E	118.66	2	59.33	1.47	0.250	2.63
F	280.65	2	140.32	8.75	0.001	6.02	F	745.32	2	372.66	9.22	0.001	16.5
Error	400.92	25	16.04			8.6	Error	1011	25	40.44			22.38
Lack-of-Fit	375.52	22	17.07	2.02	0.311	8.05		1010.62	22	45.94	357	0.000	22.37
Pure Error	25.39	3	8.46			0.54		0.39	3	0.13			0.01
Total	4663.98	35				100	Total	4517.04	35				100
R^2=0.9140		**$R^2_{(pred)}$=0.8797**		**$R^2_{(adj)}$=0.8218**			**R^2=0.5359**		**$R^2_{(pred)}$=0.6867**		**$R^2_{(adj)}$=0.5359**		

3.4.4. pH effect

As given in Figure 2(a), lower pH improved better removal of COD than a higher pH level; the highest S/N ratio was obtained at pH 2 under acidic conditions. The pH of the solution influenced the electrostatic attraction and repulsion of sono-photocatalyst which resulted with decreasing in the COD removal rate at higher pH values (Wei *et al.*, 2021). Previous research stated that the pH value of point of zero charges (pH_{zpc}) of the TiO_2 and ZnO were approximately ≈ 6.50 and 9.0, respectively indicating that the surface of the TiO_2 and ZnO will be positively charged in an acidic medium (pH<6.50 and pH<9.0) while the catalyst's surface will carry negative charges in alkaline medium (pH>6.5). Therefore, at the initial pH of 2, while the photocatalyst surface is positively charged by absorbing H^+ ions, the pollutant molecules in the poultry slaughterhouse wastewater will be negatively charged and decomposed rapidly (Soltani *et al.*, 2016). Further, in acidic

media (2.59 V at pH 0), the oxidizing potential of HO. is higher than in alkaline media (1.64 V at pH 14) (Mullapudi *et al.*, 2020). Hence, the main reason for the marginal COD decreases at higher pH values could be result of lower oxidation potential and generation rate of hydroxyl radicals (Ayare and Gogate, 2020). On the other hand, the maximum O&G removal was obtained at pH 6 (close to neutral pH) given in Figure 2(b) ($F=29.93$, $p=0.000$, $p<\alpha$). Potrich *et al.*, (2022) stated in their study that O&G removal from raw poultry slaughterhouse wastewater was 99% for the iron electrode and 97% for the aluminum electrode under a 6.2 pH and a time of 20 min.

3.4.5. H_2O_2 effect

H_2O_2 is a strong oxidizing agent, although it increases the rate of photo-oxidation, as seen in Figure 2(a), it could not have a statistically significant effect on the COD removal efficiency ($F=1.33$, $p=0.282$, $p>\alpha$). Due to the scavenging effect that is given in the following equation, the excess H_2O_2 would react with HO. and COD removal is inhibited (Patidar and Srivastava, 2021):

$$H_2O_2 + HO. \rightarrow H_2O + HO_2^{\bullet} \quad (3.3)$$

$$HO_2^{\bullet} + HO. \rightarrow H_2O + O_2 \quad (3.4)$$

However, combining of SPC process with H_2O_2 enhanced the degradation of O&G at 5 mM as shown in Figure 2(b). An ultrasound would enhance O&G degradation by dissociation of hydrogen peroxide into (HO.) radicals (Hinge *et al.*, 2016). The rate of degradation falls from 5 mM to 10 mM because after 5 mM due to the scavenging effect rather than supplying additional radicals (Mishra and Gogate, 2011).

3.4.6. Operation time effect

Operation time is one of the most effective factor in the COD and O&G removals by SPC method as illustrated in Figure 2(a-b) and Table 6 ($p=0.001$, $p<\alpha$). When the operation time of SPC process increased from 30 to 105 minutes due to higher generation of hydroxyl radicals, sharply decreased trends in COD and O&G removals were achieved, while the COD removal performance reached a maximum of 180 minutes. Also, the S/N of the O&G removal increased from 105 min to 180 min due to possible degradation of intermediate products and oil molecules. Ultrasound could be considered an alternative method that enables and accelerates to degrade of high organic strength wastewater for the first time combined with photocatalyst and UV irradiation to treat PSWW and this is consistent with work done by Abdelhay *et al.*, (2020) reported that the removal efficiency of COD from PSWW continued to increase during the sonication time (180 min). Çancı and Kılıç (2020) declared that the COD removal rate from rose processing wastewater decreased with increased reaction time due to the formation of colored intermediates as a result of oxidation. In addition, the reaction rate was reduced because of competition between these colored intermediates and main molecules. According to obtained results, the recalcitrant target compounds could be decomposed in the first 30 min by combining ultrasound and photocatalysis processes. However, the maximum COD removal efficiency was obtained at 180 min which proved the necessity of a long time for the degradation of generated high concentration of intermediate products that cannot be further oxidized by HO. radicals, thus, accumulated in the system (Al-Bsoul *et al.*, 2020). Furthermore, as given in Table 3(b), ultrasound enabled to break of O&G besides oxidation and destruction of aromatic compounds in PSWW for 30 minutes in the presence of photocatalyst and UV irradiation. It has been observed that the ultrasound process combined with the photocatalysis process shortens the oil grease removal time from PSWW. Coha *et al.*, (2021) explained in their study that radical-radical recombination and dissipation of ultrasonic energy are improved by the elevated concentrations of reactive radicals such as HO., $H^{\bullet}$, $O_2^{\bullet}$, etc. Nevertheless, such recombination may be inhibited and secondary radicals such as $CO_3^{\bullet-}$, $Cl_2^{\bullet-}$and $^{\bullet}NO_2$ may be produced that degrade pollutants and may form harmful byproducts by the increased concentration of anions. In this study, as shown in Figure 2(b), the performance of the SPC to remove O&G from PSWW could be thought to reduce the production of secondary pollutants and by-products as a result of a breakdown of oil molecules. Emerick *et al.*, (2020) indicated in their study that 90% of O&G in swine slaughterhouse wastewater was removed by electrocoagulation-flotation (ECF) using an Al electrode in 60 minutes, although 97.5% of O&G was removed by ultrasound and electrocoagulation-flotation (ECF/US) treatment in 25 min. The ECF treatment performance and O&G removal rate were increased by ultrasound irradiation because free radicals (HO., $H^{\bullet}$, $O_2^{\bullet}$) that are formed by ultrasound power helped to degrade organic pollutants (Emerick *et al.*, 2020).

4. Conclusion

In this work, for the first time, the removal efficiencies of COD and oil and grease from PSWW were conducted by a hybrid technology sono-photocatalysis. Taguchi's experimental design based on an L_{36} orthogonal array (OA) was adequately applied to optimize the process. The key results of this study could be summarized as:

- The synergy index value for the combined US/UVC_{254}/ZnO was attributed to 1.42 which performed higher oxidation performance of PSWW when compared with individual advanced oxidation processes.
- The optimum conditions obtained from Taguchi experiments for the SPC process under the following conditions: 2.5 g/L ZnO under UVC_{254} at pH 2, 180 min for COD removal; for O&G removal, they were 1.5 g/L ZnO at pH 6 under UVC_{254}, with 5 mmol/L of H_2O_2, and 30 min. With these optimum conditions, the best attained COD and O&G removal yields were 54% and 99%, respectively. Since the allowable COD and O&G concentrations for slaughterhouses according to Turkish legislation are 250 mg/L and 30 mg/L, respectively for a composite sample of 2h, hence, this step of hybrid treatment should be implemented in the primary treatment of recalcitrant

organic substances or tertiary treatment process for the complete organic pollutants.

- According to the ANOVA results, while catalyst type was of great importance in COD removal yield, pH had the most significance in O&G removal, for the SPC process.
- ZnO showed an excellent COD and O&G removal performance in comparison to the TiO_2 due to absorption of more light quanta as the quantum efficiency by adsorption and photocatalysis mechanisms. Further, UVC radiation showed statistically significant degradation performance in comparison with UVA owing to shorter wavelengths with higher energy. The presence of H_2O_2 performed a slight effect on the enhancement of O&G removal from PSWW, although COD removal efficiency decreased due to the scavenging effect in the presence of H_2O_2.
- The maximum COD removal efficiency was obtained at 180 min which proved the necessity of a long time for the degradation of generated high concentration of intermediate products that cannot be further oxidized by HO. radicals, thus, accumulated in the system. Ultrasound enabled to break of O&G and shortened the removal times besides oxidation and destruction of aromatic compounds in PSWW for 30 minutes in the presence of photocatalyst and UV irradiation.

Acknowledgments

The authors would like to extend their sincere gratitude to the Bolu Abant Izzet Baysal University Scientific Research Projects Coordination, Turkey, for its funding of this research, project number 2021.09.02.1498.

References

Abbas Z.I., Abbas A.S. (2021), Optimization of the electro-Fenton process for COD reduction from refinery wastewater, *Environmental Engineering and Management Journal*, **19**, 2029-2037.

Abdelhay A., Othman A.A., Absoul A. (2020), Treatment of slaughterhouse wastewater using high-frequency ultrasound: optimization of operating conditions by RSM, *Environmental Technology*, **42**, 4170-4178.

Abdurahman M.H., Abdullah A.Z., Shoparwe N.F. (2021), A comprehensive review on sonocatalytic, photocatalytic, and sonophotocatalytic processes for the degradation of antibiotics in water: Synergistic mechanism and degradation pathway, *Chemical Engineering Journal*, **413**, 127412.

Adar E., Acar F.N. (2021), Adsorption of textile wastewater containing triple dye on the garden soil: optimisation and modelling by Taguchi method, *International Journal of Environmental Analytical Chemistry*, (in press).

Ahmedchekkat F., Medjram M.S., Chiha M., Al-Bsoul A.M. (2011), Sonophotocatalytic degradation of Rhodamine B using a novel reactor geometry: Effect of operating conditions, *Chemical Engineering Journal*, **178**, 244– 251.

Al-Bsoul A., Al-Shannag M., Tawalbeh M., Al-Taani A.A., Lafi W.K., Al-Othman A., Alsheyab M. (2020), Optimal conditions for olive mill wastewater treatment using ultrasound and advanced oxidation processes, *Science of the Total Environment*, **700**, 134576.

APHA, AWWA and WEF. (2012), Standard Methods for the Examination of Water & Wastewater, 22nd Edition. Washington DC: American Public Health Association.

Asha R.C., Kumar M. (2015), Photocatalytic degradation of poultry wastewater using activated carbon-supported titanium dioxide, *Desalination and Water Treatment*, **54**, 3279-3290.

Ayare S.D., Gogate P.R. (2020), Sonophotocatalytic oxidation based treatment of phthalocyanine pigment containing industrial wastewater intensified using oxidising agents, *Separation and Purification Technology*, **233**, 115979.

Aydiner C., Mert B.K., Dogan E.C., Yatmaz H.C., Dagli S., Aksu S., Tilki Y.M., Goren A.Y., Balci E. (2019), Novel hybrid treatments of textile wastewater by membrane oxidation reactor: Performance investigations, optimizations and efficiency comparisons, *Science of the Total Environment*, **683**, 411–426.

Babu S.G., Karthik P., John M.C., Lakhera S.K., Ashokkumar M., Khim J., Neppolian B. (2019), Synergistic effect of sono-photocatalytic process for the degradation of organic pollutants using CuO-TiO_2/rGO, *Ultrasonic Sonochemistry*, **50**, 218–223.

Bingo M.N, Njoya M., Basitere M., Ntwampe S.K.O., Kaskote E. (2021), Performance evaluation of an integrated multi-stage poultry slaughterhouse wastewater treatment system, *Journal of Water Process Engineering*, **43**, 102309.

Boutra B., Sebti A., Trari M. (2021), Photocatalytic Treatment of Synthetic and Real Textile Wastewater Using Zinc Oxide Under the Action of Sunlight, *Theoretical and Experimental Chemistry*, **57**, 226-236.

Bushnaq Z. (2006), Evaluation of UVA, UVB and UVC Photolysis and Photocatalysis for the Removal of Atrazine from Contaminated Water, MSc Thesis, School of Engineering, University of Rmit.

Bustillo-Lecompte C.F., Ghafoori S., Mehrvar M. (2016), Photochemical degradation of an actual slaughterhouse wastewater by continuous UV/H_2O_2 photoreactor with recycle, *Journal of Environmental Chemical Engineering*, **4**, 719–732.

Çancı M.B., Kılıç M. (2020), Treatment of Rose Processing Wastewater by Sunlight/TiO_2 Photocatalysis Process, *Bilge International Journal of Science and Technology Research*, **4**, 1-16.

Cao S.T., Tran H.P., Le H.T.T., Bui H.P.K., Nguyen G.T.H., Nguyen L.T., Nguyen B.T., Luong A.D. (2021), Impacts of effluent from different livestock farm types (pig, cow, and poultry) on surrounding water quality: a comprehensive assessment using individual parameter evaluation method and water quality indices, *Environmental Science and Pollution Research*, **28**, 50302–50315.

Coha M., Farinelli G., Tiraferri A., Minella M., Vione D. (2021), Advanced oxidation processes in the removal of organic substances from produced water: Potential, configurations, and research needs, *Chemical Engineering Journal*, **414**, 128668.

Cui H., Yu J., Zhu X., Cui Y., Ji C., Zhang C., Xue J., Jia X., Qin S., Li R. (2021), Advanced treatment of chicken farm flushing wastewater by integrating Fenton oxidation and algal cultivation process for algal growth and nutrients removal, *Journal of Environmental Management*, **298**, 113543.

Cui Y., Xu G., Liu Y. (2014), Oil sorption mechanism and capability of cattail fiber assembly, *Journal of Industrial Textiles*, **43**, 330–337.

Dyosile P.A., CMdladla C., Njoya M., Ntwampe S.K.O., Kaskote E. (2021), Assessment of an Integrated and Sustainable

Multistage System for the Treatment of Poultry Slaughterhouse Wastewater, *Membranes*, **11**, 582.

Emerick T., Vieira J.L., Silveira M.H.L., João J.J. (2020), Advanced treatment of chicken farm flushing wastewater by integrating Fenton oxidation and algal cultivation process for algal growth and nutrients removal, *Journal of Environmental Management*, **298**, 113543.

Fan G., Yang S., Du B., Luo J., Lin X., Li X. (2022), Sono-photo hybrid process for the synergistic degradation of levofloxacin by $FeVO_4$/$BiVO_4$: Mechanisms and kinetics, *Environmental Research*, **204**, 112032.

Fard M.B., Mirbagheri S.A., Pendashteh A. (2020), Removal of TCOD and phosphate from slaughterhouse wastewater using Fenton as a post-treatment of an UASB reactor, *Journal of Environmental Health Science and Engineering*, **18**, 413–422.

Fatima F., Du H., Kommalapati R.R. (2021), Treatment of Poultry Slaughterhouse Wastewater with Membrane Technologies: A Review, *Water*, **13**, 1905.

Fdez-Sanromán A., Martinez-Treinta R., Pazos M., Rosales E., Sanromán M.Á. (2021), Heterogeneous Electro-Fenton-like Designs for the Disposal of 2-Phenylphenol from Water, *Applied Sciences*, **11**, 12103.

Garcia B.B., Lourinho G., Romano P., Brito P.S.D. (2020), Photocatalytic degradation of swine wastewater on aqueous TiO_2 suspensions: optimization and modeling via Box-Behnken design, *Heliyon*, **6**, 03293.

Gaur R.S., Cai L., Tuovinen O.H., Mancl K.M. (2010), Pretreatment of turkey fat-containing wastewater in coarse sand and gravel/coarse sand bioreactors, *Bioresource Technology*, **101**, 1106–1110.

Gole V.L., Priya A., Danao S.P. (2017), Decolorization of brilliant green dye using immersed lamp sonophotocatalytic reactor, *Applied Water Science*, **7**, 4237–4245.

Hapeshi E., Fotiou I., Fatta-Kassinos D. (2013), Sonophotocatalytic treatment of ofloxacin in secondary treated effluent and elucidation of its transformation products, *Chemical Engineering Journal*, **224**, 96–105.

Hilares R.T., Atoche-Garay D.F., Pagaza D.A.P., Ahmed M.A., Andrade G.J.C., Santos J.C. (2021), Promising physicochemical technologies for poultry slaughterhouse wastewater treatment: A critical review, *Journal of Environmental Chemical Engineering*, **9**, 105174.

Jyothi K.P., Yesodharan S., Yesodharan E.P. (2015), Sono-, photo- and sonophotocatalytic decontamination of organic pollutants in water: studies on the lack of correlation between pollutant degradation and concurrently formed H_2O_2, *Current Science*, **109**, 189-195.

Kakavandi B., Ahmadi M. (2019), Efficient treatment of saline recalcitrant petrochemical wastewater using heterogeneous UV-assisted sono-Fenton process, *Ultrasonics Sonochemistry*, **56**, 25–36.

Karim A.V., Shriwastav A. (2020), Degradation of amoxicillin with sono, photo, and sonophotocatalytic oxidation under low-frequency ultrasound and visible light, *Environmental Research*, **200**, 111515.

Khan M.F., Cazzato G., Saleemi H.A., Macadangdang Jr R.R., Aftab M.N., Ismail M., Khalid H., Ali S., Bakhtiar S.H., Ismail A., Zahid M. (2022), Sonophotocatalytic degradation of organic pollutant under visible light over Pt decorated CeO_2: Role of ultrasonic waves for unprecedented degradation, *Journal of Molecular Structure*, **1247**, 131397.

Khitab F., Shah J., Jan M.R. (2022), Systematic assessment of visible light driven photocatalysts for the removal of cefixime in aqueous solution sonophotocatalytically, *International Journal of Environmental Analytical Chemistry*, (in press).

Liang H., Esmaeili H. (2021), Application of nanomaterials for demulsification of oily wastewater: A review study, *Environmental Technology & Innovation*, **22**, 101498.

Mishra K.P., Gogate P.R. (2011), Intensification of degradation of aqueous solutions of rhodamine B using sonochemical reactors at operating capacity of 7 L, *Journal of Environmental Management*, **92**, 1972-1977.

Moortel W.V., Kamali M., Sniegowski K., Braeken L., Degrève J., Luyten J., Dewil R. (2020), How Photocatalyst Dosage and Ultrasound Application Influence the Photocatalytic Degradation Rate of Phenol in Water: Elucidating the Mechanisms Behind, *water*, **12**, 1672.

Mullapudi V.B.K., Salveru A., Kora A.J. (2020), An in-house UV-photolysis setup for the rapid degradation of both cationic and anionic dyes in dynamic mode through UV/H_2O_2-based advanced oxidation process, *International Journal of Environmental Analytical Chemistry*.

Ngobeni P.V., Basitere M., Thole A. (2022), Treatment of poultry slaughterhouse wastewater using electrocoagulation: a review, *Water Practice & Technology*, **17**, 38-59.

Patidar R., Srivastava V.C. (2021), Mechanistic and kinetic insights of synergistic mineralization of ofloxacin using a sono-photo hybrid process, *Chemical Engineering Journal*, **403**,125736.

Poblete R., Cortes E., Salihoglu G., Salihoglu N.K. (2020), Ultrasound and heterogeneous photocatalysis for the treatment of vinasse from pisco production, *Ultrasonic Sonochemistry*, **61**, 104825.

Potrich M.C., de Souza Almeida Duarte E., de Souza Sikora M., Costa da Rocha R.D. (2020), Electrocoagulation for nutrients removal in the slaughterhouse wastewater: comparison between iron and aluminum electrodes treatment, *Environmental Technology*, **43**, 751-765.

Potrich M.C., Duarte E.S.A., Sikora M.S., Rocha R.D.C. (2020), Electrocoagulation for nutrients removal in the slaughterhouse wastewater: comparison between iron and aluminum electrodes treatment, *Environmental Technology*, **43**, 751-765.

Samsudin M.F.R., Jayabalan P.J., Ong W.J., Ng Y.H., Sufi S. (2019), Photocatalytic degradation of real industrial poultry wastewater via platinum decorated $BiVO_4$/g-C_3N_4 photocatalyst under solar light irradiation, *Journal of Photochemistry & Photobiology A: Chemistry*, **378**, 46–56.

Silva A.M.T., Nouli E., Carmo-Apolinário Â.C., Xekoukoulotakis N.P., Mantzavinos D. (2007), Sonophotocatalytic/H_2O_2 degradation of phenolic compounds in agro-industrial effluent, *Catalysis Today*, **124**, 232–239

Sohrabi M.R., Khavaran A., Shariati S., Shariati S. (2017), Removal of Carmoisine edible dye by Fenton and photo Fenton processes using Taguchi orthogonal array design, *Arabian Journal of Chemistry*, **10**, S3523–S3531.

Soltani R.D.C., Jorfi S., Safari M., Rajaei M.-S. (2016), Enhanced sonocatalysis of textile wastewater using bentonite-supported ZnO nanoparticles: Response surface methodological approach, *Journal of Environmental Management*, **179**, 47-57.

Stando K., Kasprzyk P., Felis E., Bajkacz S. (2021), Heterogeneous Photocatalysis of Metronidazole in Aquatic Samples, *molecule*s, **26**, 7612.

Steven T., Nawaz R., Sahrin N.T., Lee K.M., Bianchi C.L., Kait C.F. (2021), H_2O_2-assisted Sonophotocatalytic Degradation of Diclofenac using a Visible Light-Active Flower-like Micron-

sized TiO_2 Photocatalyst, *Malaysian Journal of Chemistry*, **23**, 108-125.

Talinli I., Anderson G.K. (1992), Interference of hydrogen peroxide on the standard cod test, *Water Research*, **26**, 107–110.

Termtanun M. (2013), Photocatalytic degradation of pesticides using TiO_2 nanoparticles, Ph.D. Thesis, Department of Chemical and Environmental Engineering, University of Nottingham.

Wei H., Rahaman M.H., Zhao J., Li D., Zhai J. (2021), Hydrogen peroxide enhanced sonophotocatalytic degradation of acid orange 7 in aqueous solution: optimization by Box–Behnken design, *Journal of Chemical Technology and Biotechnology*, **96**, 2647–2658.

Yang Y., Wu Z.S., Yang R.P., Li Y.F., Liu X.C., Zhang L.H., Yu B. (2021), Insights into the mechanism of enhanced photocatalytic dye degradation and antibacterial activity over ternary ZnO/ZnSe/$MoSe_2$ photocatalysts under visible light irradiation, *Applied Surface Science*, **539**, 148220.

Yatmaz H.C., Sen U.D.K. (2018), Photocatalytic efficiencies of alternate heterogeneous catalysts: iron modified minerals and semiconductors for removal of an azo dye in solutions, *Environment Protection Engineering*, **44**, 5-17.

Yildiz Y.Ş. (2008), Optimization of Bomaplex Red CR-L dye removal from aqueous solution by electrocoagulation using aluminum electrodes, *Journal of Hazardous Materials,* **153**, 194–200.

Zhang S., Pang X., Yue Z., Zhou Y., Duan H., Shen W., Li J., Liu Y., Cheng Q. (2020), Sulfonamides removed from simulated livestock and poultry breeding wastewater using an in-situ electro-Fenton process powered by photovoltaic energy, *Chemical Engineering Journal*, **397**, 125466.

Zioui D., Salazar H., Audjit L., Martins P., Lanceros-MendezS. (2019), Photocatalytic polymeric nanocomposite membrane towards oily wastewater, *Preprints*, 2019040060.